

Deposition of crystalline Ge nanoparticle films by high-pressure RF magnetron sputtering method

D Ichida¹, G Uchida², H Seo¹, K Kamataki³, N Itagaki^{1,4}, K Koga¹ and M Shiratani¹

¹ Graduate School of Information Science and Electrical Engineering, Kyushu University, 744 Motooka, Nishi-ku, Fukuoka, 819-0395, Japan

² Jointing and Welding Reserch Institute, Osaka University, 11-1 Mihogaoka, Ibaraki, Osaka, 567-0047, Japan

³ Faculty of Arts and Science, Kyushu University, 744 Motooka, Nishi-ku, Fukuoka, 819-0395, Japan

⁴ PRESTO Japan Science and Technology Agency, Gobancho, Chiyoda-ku, Tokyo, 102-0076, Japan

E-mail: d.ichida@plasma.ed.kyushu-u.ac.jp

Abstract. We report here deposition of crystalline Ge nanoparticle films using a radio frequency magnetron sputtering method in argon and hydrogen gas mixture under a high pressure condition. The size of Ge nanoparticles is deduced to be 6.3-6.4 nm from the peak frequency shift of Raman spectra. Raman and X-ray diffraction spectra show that the films are crystalline. The film crystallinity strongly depends on substrate temperature (T_s). Highly crystalline Ge nanoparticle films are successfully fabricated at $T_s = 180^\circ\text{C}$.

1. Introduction

Semiconductor quantum-dot (QD) films have attracted much attention because of their application to high efficiency solar cells [1-3]. The unique characteristics of QDs such as tunable band gap and high multiple exciton generation (MEG) yield are expected to enhance the energy conversion efficiency above the Shockley and Queisser limit of 33% [4]. MEG can produce more than two excitons by one incident photon and represents a promising route to increase solar conversion efficiencies in single-junction photovoltaic cells. Our interest has been motivated by QD solar cells using Si and Ge nanoparticles [5-9], because Si and Ge are important materials of current electronics and solar cell industries. Ge QDs have more outstanding quantum confinement effects than Si QDs due to the larger excitonic Bohr radius of 24.3 nm for Ge QDs than 4.9 nm for Si ones [10-12]. Ge has also an inherent advantage over Si since Ge is known to exhibit much larger absorption coefficient in infrared light region than Si, and a high power conversion efficiency is expected for high solar light absorption.

In this study, we report fabrication of Ge QD films using Ge nanoparticles, where a high pressure rf magnetron sputtering method is applied to the deposition of Ge QD films with high crystallinity. First, we describe optical emission spectroscopy (OES) in argon and hydrogen gas mixture discharge plasma. Then, we present Raman and X-ray diffraction spectra of deposited Ge nanoparticle films deposited using a high pressure magnetron sputtering method.



2. Experimental

Figure 1 shows a schematic of experimental apparatus. Ge nanoparticle films were fabricated using 13.56 MHz RF magnetron sputtering process in an Ar and H₂ gas mixture under a high pressure condition of 200 Pa. At such high pressure, the mean free pass of Ge atoms is as short as the order of micrometer, and gas-phase Ge nanoparticle formation is possible. The fabricated Ge nanoparticles were transported to the quartz glass substrate located at 50 mm from the cathode by neutral gas flow. Ar and H₂ gas mixture were supplied at total flow of 133-250 sccm in the direction from the cathode to the substrate. H₂ dilution ratio $R_H = H_2/(H_2+Ar)$ was set in 20 %. The RF magnetron sputtering discharge plasma was generated by applying 13.56 MHz voltage to the powered electrode. The discharge RF power (P_{RF}) was 10-50 W. The sputtering target was a poly-crystalline Ge disk (1 inch) with a purity of 99.99 %.

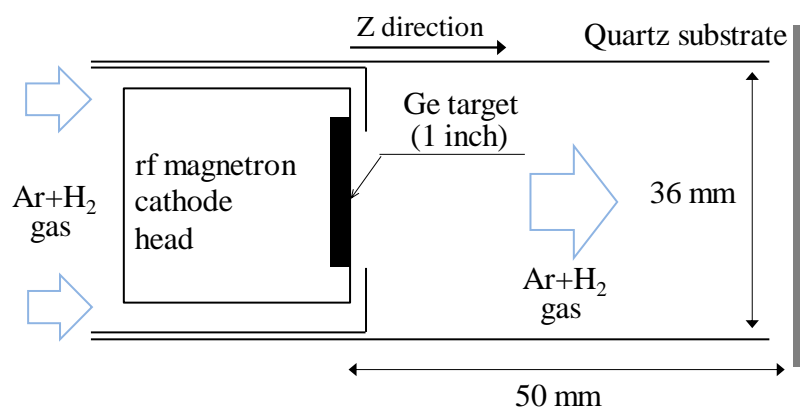


Figure 1. Experimental apparatus of high pressure RF sputtering.

3. Results and discussion

3.1. Optical emission spectroscopy of high pressure Ar/H₂ gas mixture sputtering discharge plasmas

First, we observed optical emission spectroscopy (OES) to study Ge nanoparticle production in Ar/H₂ sputtering discharge plasma. In our deposition system, Ge nanoparticles are nucleated and grow in Ar/H₂ plasma, and they are transported to the downstream region by neutral gas flow [13-15]. Therefore, the number density of Ge atoms in the plasma is an important parameter to control the particle size. Figure 2 shows a typical emission spectrum of Ar/H₂ discharge plasma. The collimator lens of 1-inch diameter was set to face to the Ge target for collecting emission light, and the intensity of light integrated in the z-direction was detected with spectrometer without setting a quartz substrate. The gas flow velocity was 0.27 m/s for the total gas flow rate of 133 sccm, and P_{RF} was 50 W. Ge 303 nm line ($I_{Ge: 303nm}$) is clearly detected in addition to Ar and H lines. As can be seen in figures 3 (a) and (b), Ge emission intensity increases linearly with P_{RF} , which is well consistent with the dependence of Ar emission intensity on P_{RF} because Ge target is mainly sputtered by Ar-ion bombardment. This results indicates that the number density Ge atoms in Ar/H₂ plasma is controlled by P_{RF} .

The emission intensity ratio of H_β 486 nm to H_α 656 nm ($I_{H: 486nm}/I_{H: 656nm}$), which corresponds to the effective electron temperature [16], is almost constant, although $I_{H: 486nm}/I_{H: 656nm}$ sharply increases at $P_{RF} = 10$ W (see figure 3(c)). The observed increase of $I_{H: 486nm}/I_{H: 656nm}$ at $P_{RF} = 10$ W is related to the shrink of plasma volume induced by lowering input power, because the electron temperature is determined by gas pressure and plasma volume [17].

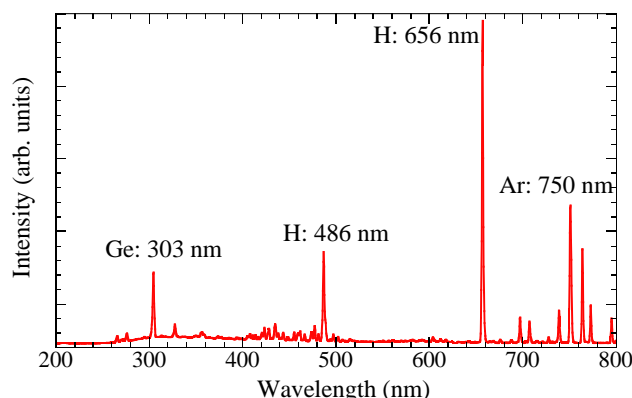


Figure 2. Typical optical emission spectrum from Ar/H₂ RF discharge plasma with the Ge sputtering target.

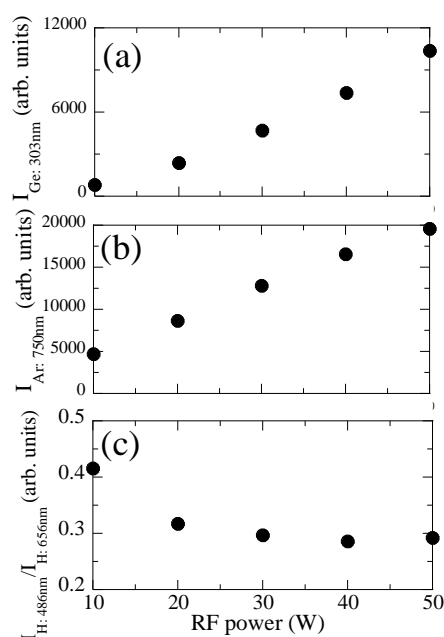


Figure 3. Discharge RF power (P_{RF}) dependence of emission intensity of (a) Ge 303 nm and (b) Ar 750 nm, and (c) emission intensity ratio of H β 486 nm to H α 656 nm.

3.2. Deposition of Ge nanoparticle films

We deposited Ge nanoparticle films using the high pressure rf magnetron sputtering method. The gas flow velocity was 0.50 m/s for the total gas flow rate of 250 sccm, and H₂ dilution ratio was 20 %. Figure 4 shows Raman spectra obtained for Ge nanoparticle films at $P_{\text{RF}} = 10, 30$ and 50 W, together with that of single crystalline Ge (c-Ge). Substrate temperature (T_s) was room one. Deposition rate increases linearly from 0.0039 to 0.042 nm/s with increasing P_{RF} from 10 to 50 W, which is well consistent with the P_{RF} dependence of $I_{\text{Ge:303nm}}$, as shown in figure 3(a). The peak frequency and the full width at half maximum (FWHM) of each peak are also given in figure 4. All films show a sharp peak at around 300 cm⁻¹, and these peaks are assigned to Ge crystals. Melting point of bulk Ge is as high as 938°C, which is much higher than gas temperature. However, the melting point of Ge nanoparticles is expected to decrease with decreasing nanoparticle size. The lower melting point for nanoparticles plays important roles to produce crystalline Ge nanoparticles. The shift of peak frequency with respect to that of reference single c-Ge depends on the nanoparticle size. There was no significant change in particle size as RF power was increased from 30 to 50 W. The particle size was deduced to be 6.3 - 6.4 nm from the relative Raman peak-shift frequency.

We also investigated the crystal orientation of Ge nanoparticle films. Figure 5 shows X-ray diffraction (XRD) pattern of Ge nanoparticle films deposited at $T_s = \text{room one}$ and 180°C. P_{RF} was 50 W. X-ray diffraction spectra of Ge nanoparticle films show crystalline structure, where the diffraction peaks appear at $2\theta = 27^\circ, 45^\circ$, and 53° corresponding to the (111), (220), and (311) crystal planes of Ge, respectively. A sharp peak with narrow width of 0.17 deg was observed for $T_s = 180^\circ\text{C}$, and high crystallinity Ge nanoparticle films were successfully fabricated by the high pressure RF sputtering process. The H₂ dilution ratio, gas flow velocity, RF power, and substrate temperature are important parameters for realizing higher crystallinity, and further experimental investigations will be carried out to obtain deep understanding of the mechanism of Ge-nanoparticle crystallization.

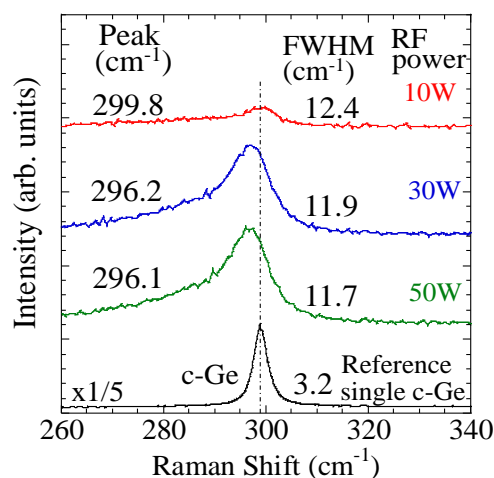


Figure 4. Raman spectra of Ge nanoparticle films showing crystalline structure. H_2 dilution ratio = 20 %, gas flow rate = 250 sccm, and substrate temperature (T_s) = room one.

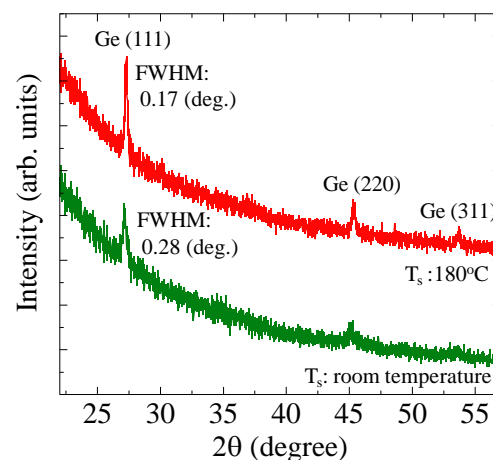


Figure 5. X-ray diffraction spectra of Ge nanoparticles deposited at substrate temperature (T_s) = room one and 180°C. Discharge RF power (P_{RF}) = 50 W, gas flow rate = 250 sccm, and H_2 dilution ratio = 20 %.

4. Conclusions

We deposited crystalline Ge nanoparticle films by the high pressure rf magnetron sputtering method. The peak frequency of Raman spectra shifts to high frequency with increasing P_{RF} , and the particle size is deduce to be 6.3 - 6.4 nm. The film crystallinity depends on T_s , and high crystalline Ge nanoparticle films are successfully fabricated at $T_s = 180^\circ\text{C}$.

Acknowledgments

This work was partly supported by the New Energy and Industrial Technology Development Organization (NEDO).

References

- [1] Nozik A J, Beard M C, Luther J M, Law M, Ellingson R J and Johnson J C 2010 *Chem. Rev.* **110** 6873
- [2] Green M A 2006 *Third Generation Photovoltaics: Advanced Solar Energy Conversion* (Berlin: Springer)
- [3] Conibeer G, Green M, Cho E, König D, Cho Y, Fangsuwannarak T, Scardera G, Pink E, Huang Y, Puzzer T, Huang S, Song D, Flynn C, Park S, Hao X and Mansfield D 2008 *Thin Solid Films* **516** 6748
- [4] Shockley W and Queisser H J 1961 *J. Appl. Phys.* **32** 510
- [5] Uchida G, Yamamoto K, Kawashima Y, Sato M, Nakahara K, Kamataki K, Itagaki N, Koga K, Kondo M and Shiratani M 2011 *Phys. Status Solidi C* **8** 3017
- [6] Uchida G, Yamamoto K, Sato M, Kawashima Y, Nakahara K, Kamataki K, Itagaki N, Koga K and Shiratani M 2012 *Jpn. J. Appl. Phys.* **51** 01AD05
- [7] Uchida G, Sato M, Seo H, Kamataki K, Itagaki N, Koga K and Shiratani M 2013 *Thin Solid Films* **544** 93
- [8] Seo H, Wang Y, Uchida G, Kamataki K, Itagaki N, Koga K and Shiratani M 2013 *Electrochim. Acta.* **87** 213
- [9] Seo H, Wang Y, Sato M, Uchida G, Kamataki K, Itagaki N, Koga K and Shiratani M 2013 *Jpn. J. Appl. Phys.* **52** 01AD05
- [10] Fujii M, Hayashi S and Yamamoto K 1990 *Appl. Phys. Lett.* **57** 2692

- [11] Zhang B, Shrestha S, Green M A and Conibeer G 2010 *Appl. Phys. Lett.* **96** 261901
- [12] Maeda Y, Tsukamoto N, Yazawa Y, Kanemitsu Y and Masumoto Y 1991 *Appl. Phys. Lett.* **59** 3168
- [13] Shiratani M, Koga K, Iwashita S, Uchida G, Itagaki N and Kamataki K 2011 *J. Phys. D* **44** 174038
- [14] Kaneya T, Koga K, Shiratani M, Watanabe Y and Kondo M 2006 *Thin Solid Films* **506–507** 288
- [15] Koga K, Inoue T, Bando K, Iwashita S, Shiratani M and Watanabe Y 2005 *Jpn. J. Appl. Phys.* **44** 1430
- [16] Takai M, Nishimoto T, Kondo M and Matsuda A 2000 *Appl. Phys. Lett.* **77** 2828
- [17] Lieberman M A and Lichtenberg A J 1994 *PRINCIPLES OF PLASMA DISCHARGE AND MATERIALS PROCESSING* (New York: John and Wiley and Sons)